Title
Alzheimer's pathology targets distinct memory networks in the ageing brain

Journal
Brain, 142(8)

ISSN
0006-8950

Authors
Maass, Anne
Berron, David
Harrison, Theresa M
et al.

Publication Date
2019-08-01

DOI
10.1093/brain/awz154

Peer reviewed

doi:10.1093/brain/awz154 BRAIN 2019: 142; 2492–2509 | 2492

BRAIN
A JOURNAL OF NEUROLOGY

Alzheimer's pathology targets distinct memory networks in the ageing brain

Anne Maass,[1,2] David Berron,[2,3,4] Theresa M. Harrison,[1] Jenna N. Adams,[1] Renaud La Joie,[5] Suzanne Baker,[6] Taylor Mellinger,[1,5] Rachel K. Bell,[1] Kaitlin Swinnerton,[1] Ben Inglis,[7] Gil D. Rabinovici,[5,6] Emrah Düzel[2,3] and William J. Jagust[1,6]

Alzheimer's disease researchers have been intrigued by the selective regional vulnerability of the brain to amyloid-β plaques and tau neurofibrillary tangles. Post-mortem studies indicate that in ageing and Alzheimer's disease tau tangles deposit early in the transentorhinal cortex, a region located in the anterior-temporal lobe that is critical for object memory. In contrast, amyloid-β pathology seems to target a posterior-medial network that subserves spatial memory. In the current study, we tested whether anterior-temporal and posterior-medial brain regions are selectively vulnerable to tau and amyloid-β deposition in the progression from ageing to Alzheimer's disease and whether this is reflected in domain-specific behavioural deficits and neural dysfunction. ^{11}C-PiB PET and ^{18}F-flortaucipir uptake was quantified in a sample of 131 cognitively normal adults (age: 20–93 years; 47 amyloid-β-positive) and 20 amyloid-β-positive patients with mild cognitive impairment or Alzheimer's disease dementia (65–95 years). Tau burden was relatively higher in anterior-temporal regions in normal ageing and this difference was further pronounced in the presence of amyloid-β and cognitive impairment, indicating exacerbation of ageing-related processes in Alzheimer's disease. In contrast, amyloid-β deposition dominated in posterior-medial regions. A subsample of 50 cognitively normal older (26 amyloid-β-positive) and 25 young adults performed an object and scene memory task while functional MRI data were acquired. Group comparisons showed that tau-positive ($n = 18$) compared to tau-negative ($n = 32$) older adults showed lower mnemonic discrimination of object relative to scene images [$t(48) = -3.2$, $P = 0.002$]. In a multiple regression model including regional measures of both pathologies, higher anterior-temporal flortaucipir (tau) was related to relatively worse object performance ($P = 0.010$, $r = -0.376$), whereas higher posterior-medial PiB (amyloid-β) was related to worse scene performance ($P = 0.037$, $r = 0.309$). The functional MRI data revealed that tau burden (but not amyloid-β) was associated with increased task activation in both systems and a loss of functional specificity, or dedifferentiation, in posterior-medial regions. The loss of functional specificity was related to worse memory. Our study shows a regional dissociation of Alzheimer's disease pathologies to distinct memory networks. While our data are cross-sectional, they indicate that with ageing, tau deposits mainly in the anterior-temporal system, which results in deficits in mnemonic object discrimination. As Alzheimer's disease develops, amyloid-β deposits preferentially in posterior-medial regions additionally compromising scene discrimination and anterior-temporal tau deposition worsens further. Finally, our findings propose that the progression of tau pathology is linked to aberrant activation and dedifferentiation of specialized memory networks that is detrimental to memory function.

1 Helen Wills Neuroscience Institute, University of California, Berkeley, Berkeley, CA 94720, USA
2 German Center for Neurodegenerative Diseases, Magdeburg, 39120, Germany
3 Institute of Cognitive Neurology and Dementia Research, Otto-von-Guericke University, Magdeburg, 39120, Germany
4 Clinical Memory Research Unit, Department of Clinical Sciences Malmö, Lund University, Lund, Sweden
5 Memory and Aging Center, University of California, San Francisco, San Francisco, CA, USA
6 Molecular Biophysics and Integrated Bioimaging, Lawrence Berkeley National Lab, Berkeley, 94720, USA
7 Henry H. Wheeler, Jr. Brain Imaging Center, University of California, Berkeley, Berkeley, CA 94720, USA

Received November 22, 2018. Revised March 13, 2019. Accepted April 10, 2019. Advance Access publication June 14, 2019

Correspondence to: Anne Maass
DZNE Magdeburg, Leipziger Strasse 44, 39120 Magdeburg, Germany
E-mail: anne.maass@dzne.de

Keywords: memory; anterior-temporal (AT); posterior-medial (PM); tau; hyperactivation

Abbreviations: DVR = distribution volume ratio; FTP = flortaucipir; PiB = Pittsburgh compound B; SUVR = standardized uptake value ratio

Introduction

While episodic memory loss is an early sign of Alzheimer's disease, older adults also often have difficulty recalling recent events, particularly if these are similar to prior experiences (Wilson *et al.*, 2006; Burke *et al.*, 2012; Leal and Yassa, 2018). Everyday events, such as parking one's bike at a particular location, typically synthesize information about objects (e.g. type and colour of the bike) and scenes (layout of the spatial environment). The processing of these two domains is thought to rely on distinct cortical pathways that converge in the hippocampus (Ranganath and Ritchey, 2012; Inhoff and Ranganath, 2017; Kim *et al.*, 2018). Object or content processing engages an anterior-temporal system of connected regions including perirhinal cortex, amygdala, inferior temporal and fusiform gyrus as well as lateral orbitofrontal and ventral temporopolar cortex. In contrast, spatial-contextual information processing relies on a posterior-medial system that comprises parahippocampal cortex, retrosplenial cortex, precuneus, posterior cingulate cortex and ventromedial prefrontal cortex. These cortical streams are funnelled into the hippocampus mainly via the entorhinal cortex, where they are still partially segregated into anterior-lateral (objects) and postero-medial (scenes) entorhinal cortex subregions (Maass *et al.*, 2015; Schröder *et al.*, 2015; Berron *et al.*, 2018; Reagh *et al.*, 2018).

Tau pathology exhibits a stereotypical pattern that initially affects the transentorhinal cortex, the transition area between lateral entorhinal cortex and perirhinal cortex, with consequent impairment of episodic memory in ageing and Alzheimer's disease (Braak and Braak, 1997; Giannakopoulos *et al.*, 2003; Maass *et al.*, 2018). If tau spreads via neural connectivity (Kfoury *et al.*, 2012; Cope *et al.*, 2018; Franzmeier *et al.*, 2019), it is plausible that this anterior-temporal network is most affected by tau deposition in the earliest stages of progression from 'normal ageing' to Alzheimer's disease. In contrast, the earliest and predominant sites of amyloid-β accumulation are posterior-midline regions such as retrosplenial/posterior cingulate cortices and precuneus (Mormino *et al.*, 2012; Villeneuve *et al.*, 2015; Palmqvist *et al.*, 2017), composed of neural 'hubs' that are highly metabolic across the lifespan (Buckner *et al.*, 2008; Oh *et al.*, 2016). In the presence of neocortical amyloid-β plaques, tau pathology in the temporal lobe further increases but also 'spreads' to posterior-midline regions (Lockhart *et al.*, 2017; Vemuri *et al.*, 2017; Leal *et al.*, 2018) where pathologies converge. A crucial question, therefore, is whether there is a selective vulnerability of anterior-temporal and posterior-medial systems to tau and amyloid-β pathology, which might also induce selective cognitive deficits or functional changes. With the availability of tau-specific radiotracers, this question can now be directly addressed *in vivo*.

Previous MRI studies on medial temporal lobe structure (Olsen *et al.*, 2017; Yeung *et al.*, 2017; Xie *et al.*, 2018) and function (Berron *et al.*, 2018; Reagh *et al.*, 2018) indicate early deterioration of anterior-temporal regions in ageing and subjects at risk for Alzheimer's disease that is linked to deficits in object memory. The contribution of tau deposition to this process remains unknown. With regard to amyloid-β, functional MRI studies with various task conditions have reported amyloid-β-related hyperactivation in hippocampus and posterior-medial regions (Sperling *et al.*, 2009; Mormino *et al.*, 2011; Vannini *et al.*, 2012; Elman *et al.*, 2014; Huijbers *et al.*, 2014; Oh *et al.*, 2015; Leal *et al.*, 2017) that seems to reflect a failure in task-related deactivation. Recent findings from tau PET studies in cognitively unimpaired elderly subjects propose that hippocampal hyperactivity is more strongly linked to tau than amyloid-β (Marks *et al.*, 2017; Huijbers *et al.*, 2019).

Here, we first sought to quantify and compare the amount of *in vivo* tau pathology in anterior-temporal versus posterior-medial regions in ageing and Alzheimer's disease using PET. We hypothesized that tau pathology in cognitively normal older adults would be relatively restricted to anterior-temporal regions because of its onset in transentorhinal cortex. We expected tau to spread into the posterior-medial system with increasing amyloid-β load (predominant in posterior-medial regions) in typical ageing and symptomatic stages of Alzheimer's disease. Second, we tested how amyloid-β and tau pathology affect domain-specific (i.e. object versus scene) mnemonic discrimination in a smaller sample of cognitively normal older adults and young adults who underwent task functional MRI. We hypothesized that anterior-temporal tau pathology would be related to worse object discrimination and posterior-medial amyloid-β and/or tau to worse scene discrimination. Third, we tested how tau and amyloid-β pathology relate to domain-specific activation in anterior-temporal and posterior-medial regions using whole-brain functional MRI data. We expected reduced domain-specific activation in anterior-temporal regions to be related with anterior-temporal tau, whereas high amyloid-β and tau burden in

posterior-medial regions would be related to elevated task-activation.

Materials and methods

Participants

Tau PET sample

The distribution of tau accumulation in anterior-temporal versus posterior-medial regions was assessed in a sample of cognitively unimpaired adults from the Berkeley Aging Cohort Study (BACS) as well as patients from the University of California San Francisco (UCSF) Memory and Aging Center. Sample characteristics are summarized in Table 1. Participants underwent 1.5 T structural MRI, ^{18}F-FTP-PET, ^{11}C-PiB-PET (required for age $\geq$ 60 years), and neuropsychological assessment. Figure 1 shows a methods overview. Amyloid-β-positivity was based on a global cortical PiB (Pittsburgh compound B) distribution volume ratio (DVR; cut-off 1.065; adapted from Mormino *et al.*, 2012; Villeneuve *et al.*, 2015). Tau-positivity was defined by mean flortaucipir (FTP) standardized uptake value ratios (SUVR) in a $Braak_{III/IV}$ composite region (cut-off 1.26; Maass *et al.*, 2017) that covers regions from both the anterior-temporal (amygdala, fusiform gyrus, inferior temporal gyrus) and posterior-medial (parahippocampal cortex, retrosplenial cortex, posterior cingulate cortex) system. The Institutional Review Boards of all participating institutions approved the study and informed consent was obtained according to the Declaration of Helsinki from all participants or authorized representatives.

The tau PET sample comprised 18 young and middle-aged controls (20–56 years), 113 cognitively normal older adults (60–93 years; 47 amyloid-β+), as well as 20 amyloid-β+ patients (65–95 years) with mild cognitive impairment (n = 8; Albert *et al.*, 2011) or dementia due to Alzheimer's disease (n = 12; McKhann *et al.*, 2011). For BACS eligibility requirements see Maass *et al.* (2017). BACS subjects undergo annual neuropsychological testing, which includes the Visual Reproduction Test and Digit Span test from the Wechsler Memory Scale-III, and the Stroop Interference Test among others. We only included late-onset (age $\geq$65 years) patients with amnestic manifestations and excluded patients with atypical phenotypes, as we were interested in the more typical presentation of Alzheimer's disease. Only 10 young adults/middle-aged controls underwent PiB PET. The distribution of amyloid-β in anterior-temporal versus posterior-medial regions was examined in individuals with available PiB data. The young adults/middle-aged group included significantly fewer females than the cognitively normal older adults [$\chi^2(1,n = 131) = 15.0$, $P < 0.001$] and patient group [$\chi^2(1,n = 38) = 9.7$, $P = 0.002$]. The cognitively normal older adults and patients did not differ in gender or age (all P's > 13).

Functional MRI sample

A subsample of the subjects described above consisting of 55 cognitively normal older adults (60–93 years) underwent 3 T functional MRI in addition to PET, while performing a mnemonic discrimination task. Furthermore, 26 young adults (20–35 years) were scanned with functional MRI of whom six also received FTP and PiB PET. The data of one cognitively normal older adult (defective button box) and one young adult (fell asleep) with no responses were excluded prior to any analyses.

We excluded subjects with overall task performance close to chance (corrected hit rate <0.1; n = 4 older adults). This led to a sample of 50 cognitively normal older adults (26 amyloid-β+; 18 Tau+) as well as 25 young adults for analyses of behavioural data. Sample characteristics are summarized in Table 1 (right). The young adults sample included more males (60%) whereas the older adult sample had more females (62%). Gender was included as covariate in subsequent analyses. There was no difference in age or gender between amyloid-β+ and amyloid-β−, or Tau+ and Tau− cognitively

Table 1 Sample characteristics

	Tau PET sample				Functional MRI subsample		
Group	**YA/MA**	**OA Aβ−**	**OA Aβ+**	**AD/MCI**	**YA**	**OA Aβ−**	**OA Aβ+**
n	18	66	47	20	25	24	26
Tau+, *n* (%)	0	14 (21)	23 (49)	18 (90)	0	7 (29)	11 (42)
Age, years, range	20–56	60–93	65–86	65–95	20–35	60–93	69–85
Age, years	32 ± 12	76 ± 7	77 ± 4	74 ± 7	26 ± 4	78 ± 7	77 ± 4
Female, *n* (%)	2 (11)	39 (59)	29 (62)	12 (60)	10 (40)	15 (63%)	16 (62)
MMSE	29 ± 1	29 ± 1	29 ± 1	$25 \pm 5_1$	29 ± 1	29 ± 1	29 ± 1
Education, years	$16 \pm 2_2$	17 ± 2	16 ± 2	$17 \pm 2_1$	$16 \pm 2_6$	17 ± 2	16 ± 2
$Braak_{III/VI}$ SUVR	1.07 ± 0.09	1.17 ± 0.09	1.28 ± 0.15	2.03 ± 0.69	$1.04 \pm 0.06_{19}$	1.17 ± 0.10	1.26 ± 0.15
Global PiB DVR	$0.98 \pm 0.02_8$	1.02 ± 0.03	1.34 ± 0.25	$1.68 \pm 0.21_1$[a]	$0.98 \pm 0.02_{19}$	$1.01 \pm 0.02_1$[a]	1.30 ± 0.25
APOE ε4 carrier, *n* (%)	5_4 (36)	5_5 (8)	24_4 (56)	10_6 (71)	3_{19} (50)	8_1 (35)	15_2 (63)

Unless otherwise stated variables denote mean ± SD. Subscripts denote number of missing values. Subjects in the functional MRI sample are also part of the larger Tau PET sample but included additional young adults (YA) without PET. Individuals were classified as amyloid-β+ if PiB DVR retention in neocortical region exceeded 1.065.

All Alzheimer's disease/mild cognitive impairment (AD/MCI) patients were amyloid-β+. Two patients with mild cognitive impairment did not exceed our threshold for tau-positivity and would—according to the recently proposed NIA-AA Research Framework (Jack *et al.*, 2018)—be classified as 'Alzheimer's disease-pathological change'. Tau positivity was defined by a mean FTP SUVR after partial volume correction in a $Braak_{III/IV}$ stage composite region (SUVR $\geq$ 1.26). Percentages are based on number of valid cases.

[a]For one patient and one older adult (OA) from the functional MRI sample only PiB SUVR was (see 'Materials and methods' section for details).

Aβ = amyloid-β; *APOE* = carriers of apolipoprotein E (*APOE*) ε4 allele; MMSE = Mini-Mental State Examination.

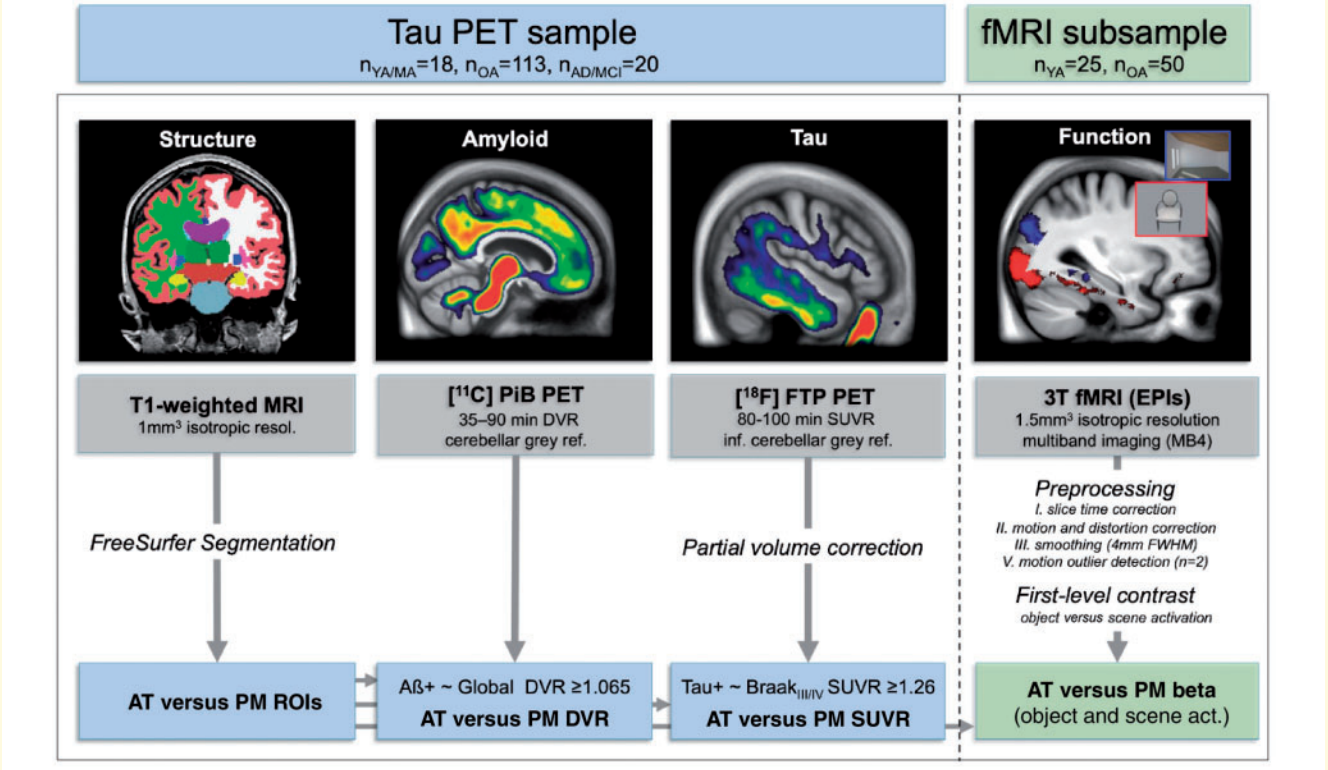

Figure 1 Overview of data and main processing steps. A group of 151 subjects spanning from youth through normal ageing to Alzheimer's disease was examined with PIB-PET (amyloid-β), FTP-PET (tau) and MRI. A subsample of 50 cognitively normal older subjects (OA) and 25 young adults (YA) (including additional subjects without PET) also underwent functional MRI while performing a mnemonic discrimination task on object and scene images (Berron *et al.*, 2018). Our main analyses on anterior-temporal (AT, in red) and posterior-medial (PM, in blue) regions were all performed in subject space using subject-specific regions of interest (ROIs) to extract measures of amyloid-β (PiB DVR), tau burden (FTP SUVR) or task activation (beta) during object or scene discrimination. Anterior-temporal and posterior-medial *a priori* regions of interest are shown in Fig. 2B. We tested effects of tau and amyloid-β by group-wise comparisons (Tau + /Tau−, amyloid-β + /amyloid-β−) and by regression analyses using continuous PET measures. MA = middle-aged adults.

normal older adults (all P's > 0.15). Although global PiB DVR and $Braak_{III/IV}$ FTP SUVR were correlated (rho = 0.36, $P = 0.009$), the proportion of Tau + did not significantly differ between amyloid-β + and amyloid-β− older adults [$\chi^2(1,n = 50) = 0.93$, $P = 0.39$].

For analyses of functional MRI data, we further excluded one young adults who was scanned as the first subject with different MRI parameters and two subjects (one young adult/one older adult) due to motion (see below), leaving 23 young and 49 cognitively normal older adults.

PET data

FTP and PiB PET acquisition and preprocessing

A detailed description of PET acquisition has been published previously (Ossenkoppele *et al.*, 2016; Schöll *et al.*, 2016). FTP images were coregistered and resliced to the structural 1.5 T MRI closest in time (see below). We created FTP SUVR images based on mean uptake over 80–100 min post-injection normalized by mean inferior cerebellar grey matter uptake (Baker *et al.*, 2017). SUVR images were partial volume corrected using the Geometric Transfer Matrix approach (Rousset *et al.*, 1998) on FreeSurfer-derived regions of interest as described in Baker *et al.* (2017). For voxelwise analyses, SUVR images were transformed into MNI152 space in via SPM 'normalize' and resampled to a resolution $1 \times 1 \times 1$ mm^3 without additional smoothing. For analyses in the tau PET sample we used the first acquired tau scan. For analyses in the functional MRI sample we chose the tau scan closest in time to the functional MRI scan (average Δtime: 60 ± 98 days).

Dynamic PiB PET frames were collected for 90 min post-injection. Frames were realigned, coregistered and resliced to the closest structural 1.5 T MRI. PiB DVRs were generated with Logan graphical analysis on frames corresponding to 35–90 min post-injection using a cerebellar grey matter reference region (Logan *et al.*, 1996; Price *et al.*, 2005). PiB scans were collected within 36 ± 89 days of FTP in the tau PET sample. Within the tau PET sample, one patient had no PiB DVR but only SUVR data available, and was rated positive based on a visual read. In our functional MRI sample, one cognitively normal older adult had only SUVR data (PiB SUVR = 1.13). We estimated a global DVR value of 1.02 for this subject based on the regression of PiB SUVR on DVR in the tau PET sample ($PiB\ DVR_{predicted} = PiB\ SUVR \times 0.612 + 0.330$; $r^2 = 0.980$, $P < 0.001$). For analyses on anterior-temporal and posterior-medial PiB DVR this subject was excluded. For

the functional MRI sample we used the PiB scan closest in time to the functional MRI session (average Δtime: 58 ± 75 days).

1.5 T MRI data used for PET processing pipeline

For all subjects with PET, $1 \times 1 \times 1$ mm^3 resolution T_1-weighted magnetization prepared rapid gradient echo (MPRAGE) images were acquired (see Supplementary material for details). All MPRAGE scans were processed with the FreeSurfer (v5.3.0; http://surfer.nmr.mgh.harvard.edu/) cross-sectional pipeline to derive regions of interest using the Desikan-Killiany atlas. Regions of interest were used for calculation of region-specific FTP SUVR (after partial volume correction) and PiB PET DVR measures.

3 T functional MRI data

Mnemonic discrimination task

During the functional MRI session, subjects performed a continuous recognition memory task on objects and scenes, described in detail in Berron *et al.* (2018). 'New'/'Old' responses are given for each image. Stimuli were presented in sequences of four with two new stimuli that were subsequently either identically repeated (correct response: 'old'; hit) or followed by a lure that was a similar new version (correct response: 'new'; correct rejection). The task was divided into two runs, each starting and ending with 10 'scrambled noise' images with a similar luminance and colour to the task stimuli. We instructed subjects to press the 'new' button for all noise images in the beginning and the 'old' button in the end of the task. These served as 'perceptual' baseline condition for functional MRI analyses.

Stimuli were presented for 3 s in an event-related design separated by a white fixation star using Neurobehavioral Systems (https://nbs.neurobs.com). There were 128 sequences consisting of four stimuli with 32 first-repeat pairs and 32 first-lure pairs per domain (=256 trials). Prior to scanning, subjects were instructed verbally and performed 2-min of training outside the scanner. Vision was tested and corrected using magnetic resonance-compatible devices if necessary.

For behavioural analyses, we calculated proportion correct for repeats (hit rates) and lures (correct rejection rate = 1 – false alarm rate) as well as corrected hit rates (hit rates – false alarm rates) for object and scene conditions.

Data acquisition and preprocessing

Whole-brain high-resolution 3 T functional MRI data were acquired across two 13-min runs using a Multiband acceleration factor of 4. Each run comprised 318 T_2*-weighted gradient-echo echo-planar images (GE-EPI) with 1.54 mm isotropic resolution. Prior to the functional MRI session, we collected a whole-brain $1 \times 1 \times 1$ mm^3 T_1-weighted MPRAGE as well as two gradient echo images with different eco times to create a phase map for distortion correction.

For preprocessing and statistical analyses we used Statistical Parametric Mapping software (SPM, Version 12; Wellcome Trust Centre for Neuroimaging, London, UK). Preprocessing comprised slice time correction, motion and distortion correction, smoothing, and outlier volume detection. Details on imaging parameters and preprocessing are given in the Supplementary material.

3 T MPRAGE scans were processed with FreeSurfer to derive regions of interest in each subject's native space. The T_1-images were also segmented into grey matter, white matter and cerebral spinal fluid using SPM12 (default parameters) and summed to create an intracranial mask for each subject. The DARTEL-imported tissue segments were used to create an intermediate study-specific DARTEL template. The resulting flow fields served to finally normalize the structural data and the functional MRI beta-images to MNI space (resolution: $1 \times 1 \times 1$ mm^3, no smoothing). A T_1-group 'template' was calculated by averaging all warped T_1-images and used for displaying second-level results.

First-level analyses

Regressors of the general linear model (GLM) included first presentations, repeats, and lures—irrespective of response—for objects and scenes (six conditions with 32 trials) plus one regressor for the scrambled images (40 trials). Furthermore, six motion regressors were added as well as outlier volumes as single regressors. Runs were concatenated. Subject-specific intracranial masks were used for explicit masking. Models were run twice, once with a conservative implicit mask of 0.8 (=proportion of global signal; SPM-default value) for subsequent region of interest-based analyses in subject space; second with a liberal implicit mask of 0.1 for voxelwise analyses in MNI space. This was done since anterior and temporal regions are often affected by dropouts and thus do not survive conservative implicit masking (voxels set NaN). After warping to MNI space these voxels would become zero in the contrast image, which we wanted to avoid by liberal implicit masking.

After model estimation, domain-specific activation contrasts were created (object > baseline, scene > baseline, object > scene, scene > object) and further used for region of interest-based or for voxelwise analyses.

Experimental design and statistical analysis

Anterior-temporal and posterior-medial regions of interest

To quantify *in vivo* tau and amyloid-β accumulation as well as domain-specific activation in anterior-temporal and posterior-medial systems we used regions of interest selected *a priori* based on the literature (Ranganath and Ritchey, 2012; Inhoff and Ranganath, 2017). Region of interest-labels were derived from FreeSurfer, which enabled us to perform analyses in subject-space without warping and to use partial volume-corrected tau PET data. Anterior-temporal regions included amygdala, fusiform gyrus (which includes perirhinal cortex or area 36) and inferior temporal gyrus. Posterior-medial regions comprised parahippocampal gyrus (corresponds to parahippocampal cortex), isthmus cingulate (corresponds to retrosplenial cortex) and precuneus. All of these regions showed preferential object (anterior-temporal) and scene (posterior-medial) activation in our task (Supplementary Fig. 5). The FreeSurfer entorhinal cortex region of interest might be considered as anterior-temporal region since it is located in the anterior temporal lobe and preferentially activated for objects in our task.

However, the entorhinal cortex can be functionally partitioned into anterior-lateral entorhinal cortex (anterior-temporal system) and posterior-medial entorhinal cortex (posterior-medial system) subregions and we thus did not include the entorhinal cortex region of interest in our analyses.

PET group analyses

To assess the regional pattern of age-related tau accumulation, we performed voxelwise two sample *t*-tests on the warped SUVR images comparing young adults/middle-aged and cognitively normal older adults in SPM. Results were false discovery rate (FDR)-corrected at cluster level ($P_{cluster} < 0.05$) with an uncorrected voxelwise threshold of $P < 0.001$ (no explicit masking).

For region of interest-based tau PET analyses, we derived an average FTP SUVR across bilateral anterior-temporal and posterior-medial regions after partial volume correction. For amyloid-β PET measures we derived an average DVR without partial volume correction. We expected higher tau measures in anterior-temporal than posterior-medial regions in cognitively normal older adults but not young adults or patients with mild cognitive impairment/Alzheimer's disease, but higher amyloid-β measures in posterior-medial than anterior-temporal regions in cognitively normal older adults and patients. To test these hypotheses, we compared anterior-temporal versus posterior-medial PET measures within each group by means of paired *t*-tests. In addition, we tested whether the difference in uptake between anterior-temporal and posterior-medial regions of interest changed with disease progression by means of two-sample *t*-tests. Statistical analyses were performed in SPSS (IBM Corp., IBM SPSS Statistics, V24, Armonk, NY, USA).

Behavioural group analyses

We performed a mixed ANOVA to test for differences in task accuracy (proportion correct) with Task condition (repeat versus lure) and Domain (object versus scene) as within-subject factors, and the between-subject factor (i) Age group (young adults versus cognitively normal older adults); (ii) Amyloid-β group (amyloid-β+ versus amyloid-β−); and (iii) Tau group (Tau+ versus Tau−). Gender was included as covariate in all analyses and age in (ii) and (iii). We also calculated behavioural domain-specificity scores as the difference in proportion correct between object and scenes (Δproportion $correct_{Obj.-Scene}$).

Next, we tested whether continuous measures of posterior-medial PiB DVR and anterior-temporal FTP SUVR affected mnemonic discrimination performance in a GLM accounting for age and gender. These analyses were restricted to lure accuracy only, which showed differences between Tau+ and Tau− cognitively normal older adults. We hypothesized an effect of posterior-medial PiB DVR on scene and anterior-temporal FTP SUVR on object lure accuracy. We also report bivariate correlations between PET measures and lure accuracy. Spearman correlation coefficients were obtained in MATLAB (function 'partialcorr') controlling for age and gender. Reported *P*-values are not corrected for multiple comparisons.

Functional MRI data group analyses

We performed voxelwise one-sample *t*-tests separately in young and cognitively normal older adults to examine whole brain activation patterns in our task. One goal was to test whether we can replicate the anterior-temporal- and posterior-medial-specific activation patterns shown by Berron *et al.* (2018) with a different EPI-acquisition protocol in an independent sample. Contrast-images (weighted sum of betas) derived at first-level (0.1 implicit mask) were warped to MNI space via DARTEL without additional smoothing. Results were FDR-corrected at cluster-level ($P_{cluster} < 0.05$) with an uncorrected $P_{voxel} < 0.005$ using an explicit cortical mask.

For region of interest-based analyses in subject-space, we extracted mean beta-values from the contrast-images (0.8 implicit mask) for anterior-temporal and posterior-medial regions of interest. FreeSurfer regions of interest were derived via segmentation of the 3 T MPRAGE, which was coregistered and resliced to the functional data. Mixed ANOVAs were performed with Domain (object versus scene) as within-subject factor and Amyloid-β group (amyloid-β+ versus amyloid-β−) or Tau group (Tau+ versus Tau−) as between-subject factor to test for main effects of Group or Group × Domain interactions. All analyses were separately run in anterior-temporal and posterior-medial regions of interest. We did not test for Condition × Region interaction since these are considered problematic in functional MRI due to potential regional differences in the haemodynamic coupling. In addition, we also performed regression analyses with continuous measures of activation. Age and gender were included as covariates in all models.

Data availability

The data that support the findings of this study are available from the corresponding author, upon request.

Results

Tau dominates in anterior-temporal and amyloid-β in posterior-medial regions

Elevated tau tracer uptake in cognitively normal older adults relative to young/middle-aged controls (Fig. 2A) was most dominant in anterior and temporal regions (entorhinal cortex, amygdala, anterior hippocampus, inferior temporal gyrus, fusiform gyrus, temporal pole, orbitofrontal cortex) but also seen in a few posterior-medial regions (parahippocampal cortex, posterior cingulate cortex/retrosplenial cortex and precuneus).

Mean anterior-temporal and posterior-medial tau and amyloid-β PET measures derived from *a priori* regions of interest (Fig. 2B) for each diagnostic group are illustrated in Fig. 2C. Anterior-temporal regions showed higher FTP SUVR than posterior-medial regions in amyloid-β− cognitively normal older adults [$t(65) = 13.7$, $P < 0.001$], amyloid-β+ cognitively normal older adults [$t(46) = 6.1$, $P < 0.001$] and mild cognitive impairment/Alzheimer's disease patients [$t(19) = 2.8$, $P = 0.01$]. No difference was seen in young adults [$t(17) < 1$, $P \sim 1$]. The pattern was consistent across individual anterior-temporal and posterior-

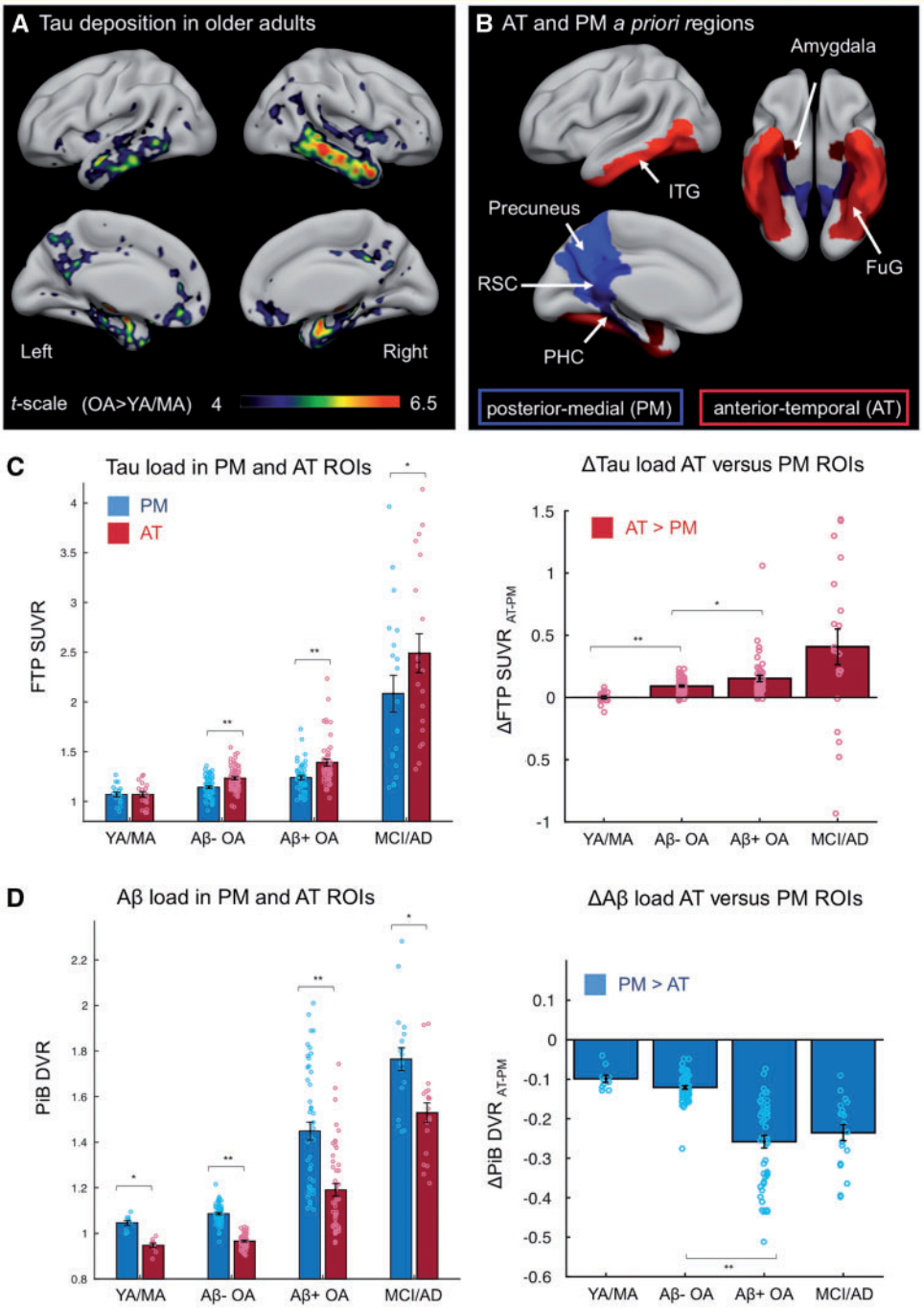

Figure 2 Tau and amyloid-β accumulation dominates in anterior-temporal and posterior-medial regions in ageing and Alzheimer's disease. (**A**) Age-related regional patterns of tau accumulation revealed by a voxelwise two-sample *t*-test on FTP tau PET scans from 113 older adults (OA) versus 18 young/middle-aged adults (YA/MA). Results are FDR corrected at cluster-level [$P_{cluster\ (FDR)} < 0.05$, $P_{voxel\ (uncorr)} < 0.001$]. No explicit mask was used. (**B**) *A priori* defined anterior-temporal (AT) regions in red comprised fusiform gyrus (FuG; including perirhinal cortex), amygdala, and inferior temporal gyrus (ITG). Posterior-medial (PM) regions in blue included parahippocampal cortex (PHC), retrosplenial cortex (RSC), and precuneus. (**C**) Mean tau PET measures in anterior-temporal and posterior-medial regions (*left*) and the anterior-temporal-posterior-medial difference in SUVR (*right*) across disease progression from 18 young adults/middle-aged, 66 amyloid-β− cognitively normal older adults, 47 amyloid-β+ cognitively normal older adults and 20 amyloid-β+ patients. FTP SUVRs were derived from FreeSurfer regions of interest after partial volume correction and averaged across regions of interest (ROIs). (**D**) Amyloid-β measures in anterior-temporal and posterior-medial regions (*left*) and the anterior-temporal-posterior-medial difference (*right*) assessed by PiB PET. $^{**}P < 0.01$; $^{*}P < 0.05$ for paired or two-sample *t*-test (uncorrected, 2-tailed); error bars denote standard error of the mean (SEM).

medial regions (Supplementary Fig. 1A). Moreover, the relative difference ΔFTP $SUVR_{AT-PM}$ (Fig. 1C) increased with disease progression from young/middle-aged adults to amyloid-β− cognitively normal older adults [$t(82) = -6.4$, $P < 0.001$] and from amyloid-β− to amyloid-β+ cognitively normal older adults [$t(111) = -2.7$, $P = 0.008$]. A further increase from amyloid-β+ older adults to patients was marginal [$t(20.2) = -1.8$, $P = 0.09$]. Within cognitively normal older adults higher global (whole brain) measures of amyloid-β and tau pathology were related to higher ΔFTP $SUVR_{AT-PM}$ difference as shown in Supplementary Fig. 1B and C.

PiB DVR showed the opposite pattern compared to FTP SUVR with higher values in posterior-medial regions of interest in all groups (all $t > 11$, all $P < 0.001$; Fig. 2). Moreover, the difference ΔPiB DVR_{AT-PM} significantly decreased from amyloid-β− to amyloid-β+ cognitively normal older adults [$t(53.9) = 8.0$, $P < 0.001$; Fig. 2D] due to a stronger PiB DVR increase in posterior-medial relative to anterior-temporal regions of interest. The difference ΔPiB DVR_{AT-PM} was only marginally lower in amyloid-β− cognitively normal older adults than young / middle-aged adults [$t(73) = -1.64$, $P = 0.10$] and similar in amyloid-β+ older controls and patients [$t(64) = -0.90$; $P = 0.37$].

As shown in Supplementary Fig. 2A and B, supplementary voxelwise analyses using functionally-defined object and scene preference masks were consistent with the region of interest-based findings. However, we chose to use native space regions of interest because the functional masks (i) did not allow us to apply partial volume correction; (ii) included early visual regions that were not relevant to our hypotheses; and (iii) suffered from substantial signal dropout in the functionally defined anterior-temporal (object) regions. To summarize, anterior-temporal regions showed higher tau PET measures than posterior-medial regions in cognitively normal older adults and symptomatic patients, and this difference increased from amyloid-β− older adults through amyloid-β+ older adults and patients. In contrast, posterior-medial regions showed higher amyloid-β PET measures in all groups, with increasing posterior-medial relative to anterior-temporal values from amyloid-β− to amyloid-β+ ageing.

Tau and amyloid-β deposition affect domain-specific mnemonic discrimination

Tau positivity relates to reduced performance on object lures

Fifty cognitively normal older and 25 young adults performed the continuous recognition memory task on object and scene images (Fig. 3A); the proportion correct is illustrated in Fig. 3B for lures and Supplementary Fig. 3 for repeats.

Cognitively normal older adults performed significantly worse than young adults on both repeat and lure stimuli, revealed by a main effect of age group [$F(1,72) = 30.7$, $P < 0.001$], and significant *post hoc* *t*-tests (Supplementary Table 1). Moreover, we found a significant Domain × Stimulus type interaction [$F(1,72) = 8.7$, $P = 0.004$] due to lower accuracy (i.e. correct rejection) for scene than object lures in both age groups. We also found a Domain × Gender interaction [$F(1,72) = 4.6$, $P = 0.034$] due to worse performance on scenes than objects in females [$t(40) = -5.6$, $P < 0.001$] with no difference in males [$t(34) = -0.98$, $P = 0.34$]. Notably, there was no interaction of Domain × Age group or Domain × Stimulus type × Age group (all F's < 1, P's > 0.6) suggesting that cognitively normal older adults performed similarly worse on both scenes and objects relative to young adults, confirming previous findings by Berron *et al.* (2018).

Within cognitively normal older adults, there were no significant differences in performance between amyloid-β+ and amyloid-β− subjects (all F's < 1.4, all P's > 0.2). However, when grouping older adults based on tau-positivity, there was a significant interaction of Tau group × Domain [$F(1,46) = 6.2$, $P = 0.016$], and Tau group × Domain × Stimulus type [$F(1,46) = 5.9$, $P = 0.019$]. *Post hoc* tests revealed that the higher accuracy for object than scene lures seen in young adults was also present in Tau− older adults [$t(31) = 5.44$, $P < 0.001$] but not in Tau+ cognitively normal older adults [$t(17) = -0.59$, $P = 0.56$] with a trend for a reduction in object lure discrimination accuracy in Tau+ compared to Tau− cognitively normal older adults [$F(1,46) = 2.9$, $P = 0.095$; GLM including covariates]. Correct response to object lures relative to scenes ($\Delta\text{proportion correct}_{Obj.-Scene}$) was significantly lower in Tau+ compared to Tau− cognitively normal older adults [$t(48) = -3.2$, $P = 0.002$; Fig. 3B]. Results were consistent for corrected hit rates [$t(48) = -2.5$, $P = 0.017$] and tau groups did not differ in repeat recognition [$F(1,46) < 1$, $P = 0.92$; Supplementary Fig. 3]. A GLM on lure discrimination including both amyloid-β and tau group confirmed the effect of tau group but did not reveal any significant Amyloid-β × Tau group interaction (Supplementary Table 2).

To summarize, domain-specific lure discrimination differed between Tau+ and Tau− cognitively normal older adults even when controlling for amyloid-β group. Specifically, Tau+ cognitively normal older adults performed worse on object lures relative to scene lures compared to Tau− older adults.

Anterior-temporal tau and posterior-medial amyloid-β differentially affect object versus scene lure discrimination

In a next step, we tested specifically whether continuous regional measures of posterior-medial amyloid-β and anterior-temporal tau were related to scene and object lure discrimination, respectively. To that end, we ran a GLM

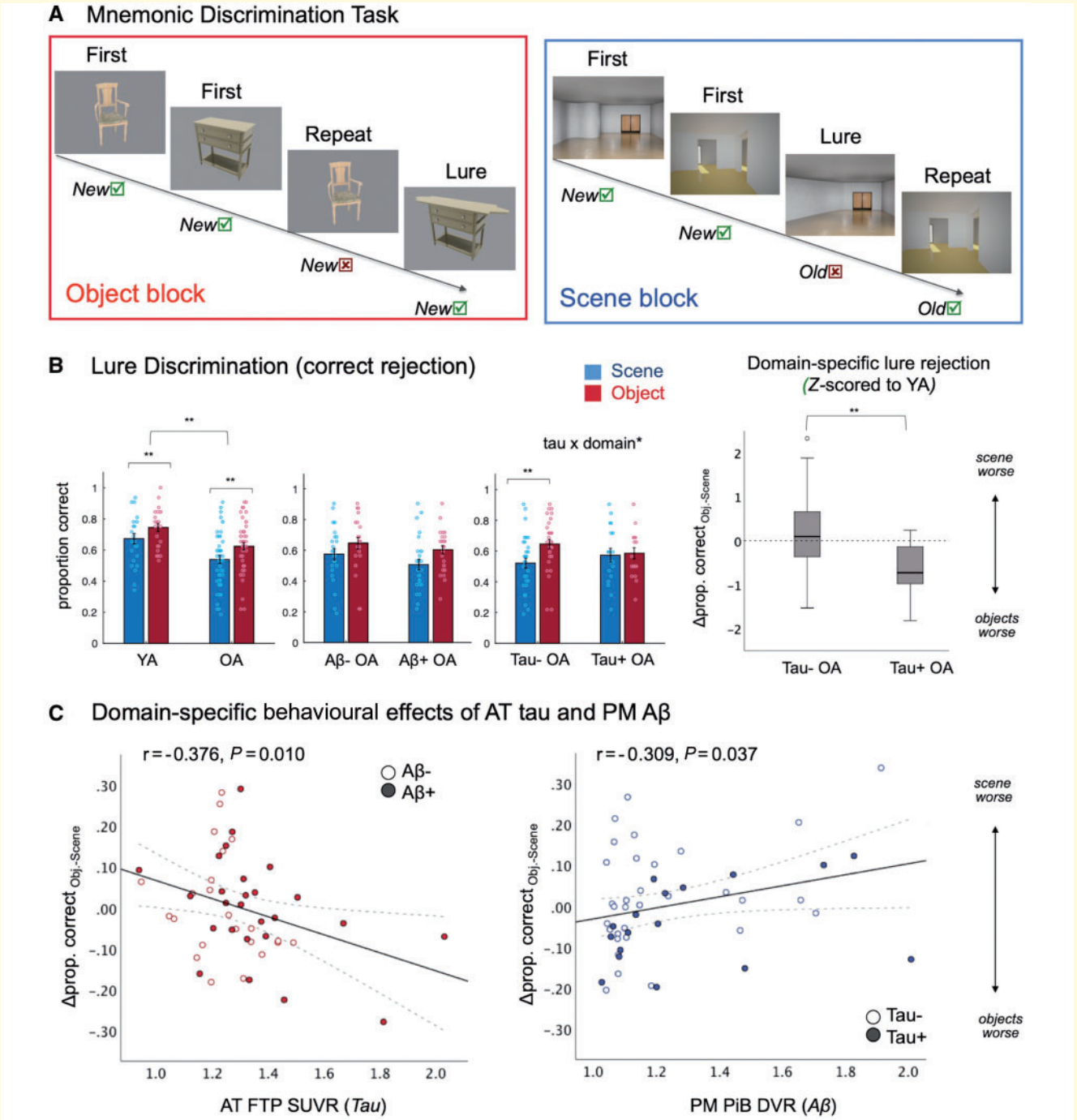

Figure 3 Tau and amyloid-β differentially affect object versus scene lure discrimination. (**A**) Trials consisted of two new stimuli that were subsequently either identically repeated (correct response: 'old'; hit) or followed by a lure, which is a very similar new version (correct response: 'new'; correct rejection). (**B**) Proportion correct for lure stimuli for objects and scenes separated by groups. Tau + cognitively normal older adults (OA) performed relatively worse on object lures (relative to scenes) compared to Tau− cognitively normal older adults (Tau × Domain interaction). See Supplementary Fig. 3 for response to repeats. YA = young adults (n = 25); OA = older adults (n = 50); $^{**}P < 0.01$; $^{*}P < 0.05$ for two-sample t-tests (uncorrected, 2-tailed); error bars denote SEM. (**C**) A multiple regression revealed that higher anterior-temporal (AT) FTP SUVR was related to worse object performance relative to scenes, whereas in the same model higher posterior-medial (PM) PiB DVR was related to worse scene performance relative to objects (n = 49; one cognitively normal older adult had only PiB SUVR). Adjusted (=residual) behavioural data are plotted adjusting for age, gender and the other PET modality. For bivariate correlations of PET measures and lure performance for objects and scenes, see Supplementary Fig. 4. Aβ = amyloid-β.

within cognitively normal older adults on lure accuracy with domain (object versus scene) as within-subjects factor and both posterior-medial PiB DVR and anterior-temporal FTP SUVR as predictors, controlling for age and gender. The interaction with domain was significant for posterior-medial PiB DVR [$F(1,44) = 4.6$, $P = 0.037$] and for anterior-temporal FTP SUVR [$F(1,44) = 7.3$, $P = 0.010$], indicating domain-specific relationships with both proteins. To test for directionality of these effects, we ran a GLM on the behavioural domain-specificity score (Δproportion $correct_{Obj.-Scene}$). As illustrated in Fig. 3C, higher anterior-temporal FTP SUVR was related to worse object performance relative to scenes [$P = 0.010$, unstandardized $B = -0.289$, standard error (SE) = 0.107, partial $\eta^2 = 0.142$, $r = -0.376$], whereas in the same model higher posterior-medial PiB DVR was related to worse scene performance relative to objects ($P = 0.037$, unstandardized $B = 0.166$, SE = 0.077, partial $\eta^2 = 0.095$, $r = 0.309$). Notably, control analyses adding posterior-medial FTP SUVR as additional covariate did not change the results. Furthermore, performing the same multiple regression with anterior-temporal PiB DVR and posterior-medial FTP SUVR did not reveal any significant effect (all F's < 2.7; all P's > 0.11).

Supplementary Fig. 4 illustrates the individual bivariate relationships of anterior-temporal FTP SUVR (Supplementary Fig. 4A) and posterior-medial PiB DVR (Supplementary Fig. 4B) with lure discrimination. Higher anterior-temporal FTP SUVR was related to worse object lure discrimination (rho = −0.29, $P = 0.047$), and higher posterior-medial PiB DVR was related to worse scene lure discrimination (rho = −0.290, $P = 0.048$), covarying for age and gender. Similar relationships were seen for the relative of amount of tau (Δanterior-temporal-posterior-medial FTP SUVR) and amyloid-β (Δposterior-medial-anterior-temporal PiB DVR). Individual regions of interest where tau measures were related to lure performance are noted in the legend of Supplementary Fig. 4.

Tau deposition affects domain-specific activation

Object versus scene conditions engage anterior-temporal versus posterior-medial systems in young and older adults

As illustrated in Fig. 4, object and scene conditions differentially engaged anterior-temporal versus posterior-medial cortical systems in both young adults (Fig. 4A) and cognitively normal older adults (Fig. 4B), which replicates previous findings by Berron *et al.* (2018). Regions that were more activated for scenes than objects included superior occipital and parietal regions, precuneus, posterior cingulate/retrosplenial cortices, parahippocampal cortex, subiculum and parts of dorsal medial prefrontal cortex. In contrast, higher activation for objects than scenes was found in middle, inferior and lateral occipital cortex, fusiform gyrus, amygdala, perirhinal cortex, insula as well as orbitofrontal cortex.

Region of interest-based analyses in subject space (bilateral mean beta-values) show that our *a priori* anterior-temporal and posterior-medial regions of interest preferentially activated for objects and scenes, respectively (Supplementary Fig. 5). Notably, voxels with low signal due to high dropouts were excluded from these analyses leading to less available data for anterior-temporal regions of interest (Supplementary Fig. 6).

Higher tau measures relate to increased task activation and reduced domain-specificity

First, we tested whether object or scene activation, relative to the perceptual baseline, in posterior-medial or anterior-temporal regions was altered in Tau+ relative to Tau− cognitively normal older adults. In posterior-medial regions of interest, there was a significant Domain × Tau group interaction [$F(1,45) = 4.7$, $P = 0.036$; Fig. 5A] on task activation. While tau groups showed similar activation levels during scene processing [$t(47) = 1.3$, $P = 0.20$], object-related activation was significantly higher in Tau+ cognitively normal older adults [$t(47) = 2.5$, $P = 0.016$]. Thus, Tau+ older adults showed reduced domain-specific activation ($\Delta beta_{Scene-Obj.}$) in posterior-medial regions of interest compared to Tau− older adults [$t(47) = -2.2$, $P = 0.032$; see also Supplementary Fig. 5A]. A main effect of tau group on posterior-medial activation was trending [$F(45,1) = 3.3$, $P = 0.074$].

In anterior-temporal regions of interest, a main effect of tau group on task activation was significant [$F(1,45) = 4.3$; $P = 0.044$; Fig. 5B]. Tau+ cognitively normal older adults showed higher activity during object [$t(47) = 2.9$, $P = 0.008$] and scene [$t(47) = 2.2$, $P = 0.033$] processing than Tau− older adults. There was no significant Domain × Tau group interaction in anterior-temporal regions of interest [$F(1,45) = 1.1$, $P = 0.30$], suggesting that task-related 'over-activation' was not domain-specific. See also Supplementary Fig. 5B for $\Delta beta_{Obj.-Scene}$ in individual anterior-temporal regions. Results were consistent when we controlled for global PiB DVR, global cortical thickness or overall task performance (mean corrected hit rate).

Next we performed the same analysis to test for differences by amyloid-β group. In posterior-medial regions a main effect of amyloid-β group on task activation was trending [$F(1,45) = 3.0$, $P = 0.090$; Fig.5A] with no significant Domain × Group interaction [$F(1,45) = 0.9$, $P = 0.35$] as seen as for tau group. In anterior-temporal regions, there was no significant main effect of amyloid-β group on activation and no Domain × Amyloid-β group interaction (all F's $\leqslant 2$, all P's > 0.16; Fig. 5B).

GLMs including both amyloid-β and tau group did not reveal any significant Amyloid-β × Tau group interaction in posterior-medial or anterior-temporal regions (Supplementary Tables 3 and 4). As previous studies have focused on hippocampus and entorhinal cortex, we performed the same analyses for these two regions that were

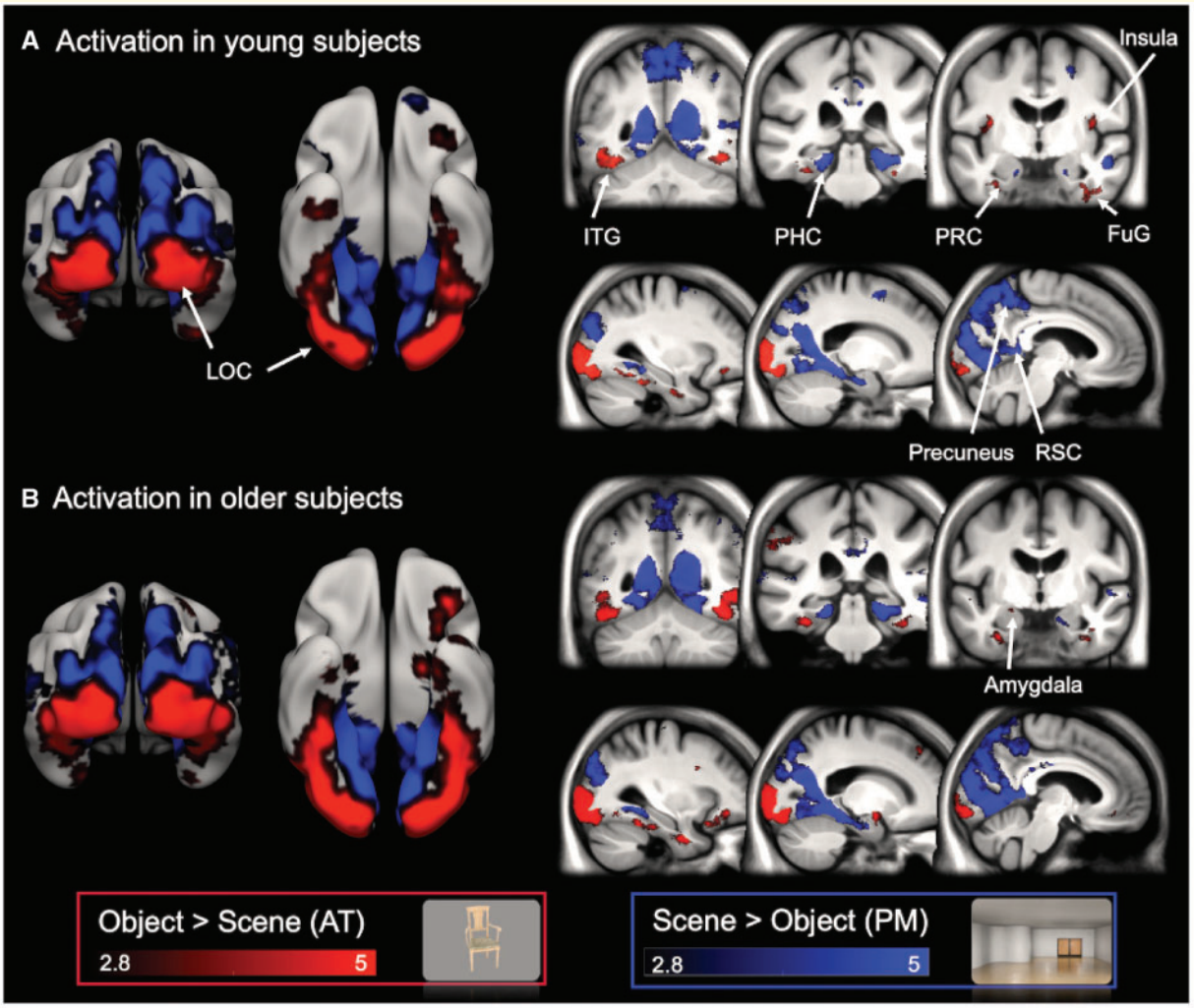

Figure 4 Whole brain domain-specific activation for young and older adults. Object versus scene conditions engage anterior-temporal (AT) versus posterior-medial (PM) systems. Scene > object (blue) and object > scene (red) one-sample *t*-test contrasts in (**A**) young ($n = 23$) and (**B**) older adults ($n = 49$). Gender was included as covariate. Results are FDR-corrected at cluster-level ($P_{cluster} < 0.05$, $P_{voxel} < 0.001$ uncorrected). Scaled *t*-values are shown overlaid on the T_1-group template. Whole-brain functional MRI data were acquired with 1.5 mm^3 isotropic resolution using multiband imaging (factor 4). FuG = fusiform gyrus; ITG = inferior temporal gyrus; LOC = lateral occipital cortex; PHC = parahippocampal cortex; PRC = perirhinal cortex; RSC = retrosplenial cortex.

not included in our anterior-temporal or posterior-medial regions of interest. There was a main effect of tau group on task activation in hippocampus [$F(1,45) = 5.9$, $P = 0.019$] but no other significant main effect of tau or amyloid-β group and no interaction with domain in hippocampus or entorhinal cortex (all F's < 2, all P's > 0.16).

To summarize, Tau+ older adults showed higher activation than Tau− older adults during both object and scene processing in anterior-temporal regions as well as hippocampus. In posterior-medial regions that usually do not or weakly activate for objects, Tau+ older adults 'over-activated' during object processing relative to Tau− older adults, resulting in diminished functional domain-specificity. This pattern was consistent across single posterior-medial regions of interest (Supplementary Fig. 4A) and results were similar when we accounted for amyloid-β.

Figure 5C further illustrates the positive relationship between object activation in posterior-medial regions of interest and continuous tau measures (rho = 0.45, $P = 0.002$) that was not present for continuous measures of amyloid-β (rho = 0.18, $P = 0.22$; Fig. 5D).

Posterior-medial tau is predicted by increased activation and global amyloid-β

We found that Tau+ cognitively normal older adults exhibited elevated task activation. Animal models have shown that increased neural activation facilitates tau propagation (Yamada *et al.*, 2014; Wu *et al.*, 2016). Recent human data indicate that amyloid-β facilitates the spread of tau out of the medial temporal lobe to posterior-medial regions (Jacobs *et al.*, 2018). As the transition from ageing to Alzheimer's disease is characterized by a 'spread' of tau

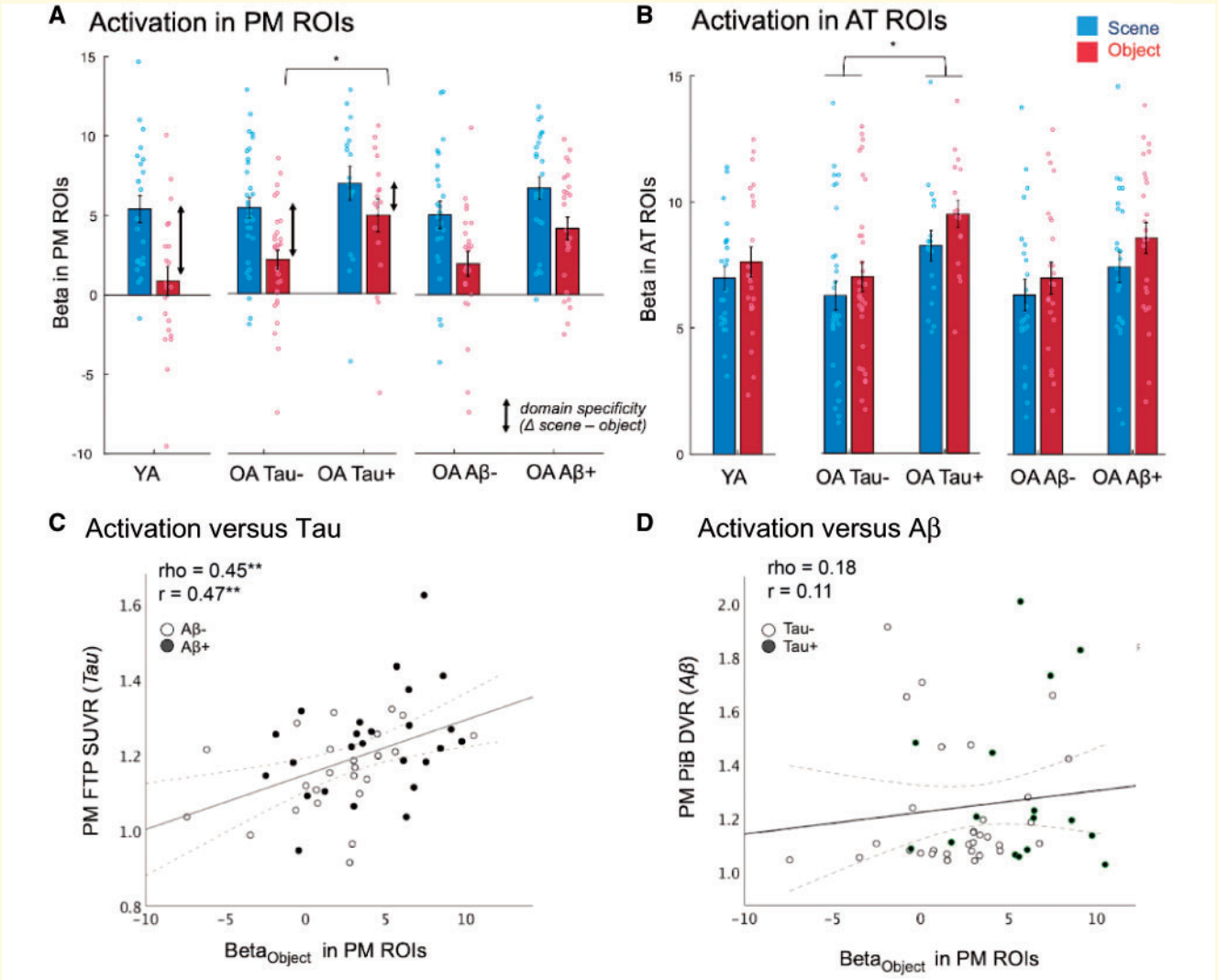

Figure 5 Higher tau measures relate to increased task activation and reduced functional domain-specificity. Mean activation (beta derived from regions of interest in subject space) for scene and object processing relative to a perceptual baseline (i.e. scrambled images) in posterior-medial (PM) (**A**) and anterior-temporal (AT) (**B**) regions for young adults as reference and cognitively normal older adults stratified by tau or amyloid-β group. See Fig. 2B for anterior-temporal and posterior-medial regions of interest. Tau + cognitively normal older adults (OA) showed object-specific over-activation in posterior-medial regions (**A**) and general over-activation in anterior-temporal regions (**B**). *$P < 0.05$ for two-sample *t*-tests. Paired *t*-test results are not denoted. Error bars are SEM. (**C**) Higher tau measures were related to higher activation—here shown for posterior-medial regions during object processing. (**D**) No such association was seen between posterior-medial amyloid-β PET measures and object activation. Both Spearman rank coefficient (rho) and Pearson coefficient (r) are reported controlling for age and gender. Raw data are plotted (not residuals). **$P < 0.01$ (uncorrected, 2-tailed). Aβ = amyloid-β; ROIs = regions of interest.

out of the anterior-temporal lobe to posterior-medial regions, we were interested specifically in contributions of activation versus amyloid-β to tau burden in these more advanced regions. We thus tested whether activation and amyloid-β independently or interactively predicted tau burden in posterior-medial regions. A stepwise regression first examined the best predictor(s) of posterior-medial FTP SUVR among activation measures (i.e. betas for object and scene processing in anterior-temporal and posterior-medial regions of interest) and global PiB DVR. The best model included object activation in posterior-medial regions of interest (Fig. 5C) and global PiB DVR as independent predictors of posterior-medial FTP SUVR as shown in Table 2 (Model 1). An interactive effect of activity with amyloid-β on posterior-medial tau was not significant (Model 2). We note that our cross-sectional data also allow the inverse interpretation that higher tau burden predicts increased activation.

Higher domain-specific activation relates to better memory performance

Finally, we examined whether the diminished functional domain-specificity in posterior-medial regions of interest

Table 2 General linear models predicting posterior-medial tau burden by activation and global amyloid-β

Model	Parameter	*B* (unstand.)	SE	t	*P*	Partial η^2	Obs. power
1	Age functional MRI	−0.003	0.003	−1.146	0.258	0.029	0.202
	Gender	0.064	0.033	1.943	0.058	0.079	0.477
	PM object activation	**0.013**	**0.004**	**3.120**	**0.003**	**0.181**	**0.862**
	Global amyloid-β	**0.178**	**0.070**	**2.539**	**0.015**	**0.128**	**0.700**
2	Age functional MRI	−0.003	0.003	−1.119	0.269	0.028	0.195
	Gender	0.067	0.033	2.013	0.050	0.086	0.503
	PM object activation	**0.013**	**0.004**	**3.126**	**0.003**	**0.185**	**0.863**
	Global amyloid-β	**0.173**	**0.070**	**2.460**	**0.018**	**0.123**	**0.672**
	Amyloid-β × PM object activation	0.013	0.017	0.793	0.432	0.014	0.121

Global amyloid-β was measured as PiB DVR across cortical regions. Activation denotes the mean beta derived from posterior-medial (PM) regions of interest for the object versus baseline contrast. A stepwise regression revealed posterior-medial object activation and global amyloid-β as best predictors of PM tau. Model 1: $F(4,44) = 6.4$, Adjusted $R^2 = 0.310$. Model 2: $F(5,43) = 5.2$, Adjusted $R^2 = 0.304$. The second model was run to test for an interactive effect of amyloid-β and activation (both variables centred) in predicting tau load. Significant variables are highlighted in bold.

seen in Tau+ cognitively normal older adults was detrimental or beneficial to cognitive performance.

We found that within cognitively normal older adults, higher domain-specific activation in posterior-medial regions ($\Delta beta_{Scene-Obj.}$) was related to better functional MRI task performance, i.e. corrected hit rates, for both objects (rho = −0.37, $P = 0.011$) and scenes (rho = −0.31, $P = 0.032$) as shown in Fig. 6A. There was no such positive association in young adults (all |rho's| < 0.36, P's > 0.09; all rho-values negative). We also tested whether the relationship between functional domain-specificity and memory performance would generalize to an independent measure of visual memory (recall and recognition in Wechsler Memory Scale) and whether it would also apply to executive function (number correct in 60 s in the Stroop Interference Test) or working memory (forward and backwards total score in Digit Span Test) assessed during the neuropsychological testing session. We found that domain-specific activation in posterior-medial regions was positively related to visual memory (immediate recall: rho = 0.37, $P = 0.010$; 20-min delayed recall: rho = 0.50, $P < 0.001$, recognition: rho = 0.37, $P = 0.011$; Fig. 6B) but not executive function (rho = −0.08, $P > 0.50$) or working memory (rho = 0.23, $P = 0.124$).

Discussion

Our data suggest a regional localization of tau and amyloid-β pathology to anterior-temporal and posterior-medial systems that is reflected in distinct behavioural deficits in object and scene mnemonic discrimination in cognitively normal older adults. More advanced tau pathology was also linked to elevated task activation and reduced functional domain-specificity of posterior-medial regions. This reduced functional domain-specificity due to object-related hyperactivation predicted worse performance in our task as well as an independent pencil-and-paper memory test. These findings are summarized in Supplementary Fig. 7.

An anterior-temporal pattern of tau accumulation in ageing is in accordance with *ex vivo* data showing that at age 60, transentorhinal tau stages are common (Braak and Braak, 1997). Surprisingly, the amount of anterior-temporal tau exceeded posterior-medial tau in patients with probable Alzheimer's disease. Although we draw longitudinal inferences from cross-sectional data, this suggests that posterior-medial regions are affected by tau later in the course of the disease and do not 'catch up' while anterior-temporal tau accumulation accelerates further. This can be explained by the relentless progression of tau pathology (Braak and Braak, 1997) that starts in transentorhinal cortex and is accelerated in the presence of amyloid-β. It is debated whether tau aggregation confined to the temporal lobe in the absence amyloid-β—also termed 'primary age-related tauopathy' (PART; Crary *et al.*, 2014)—and Alzheimer's disease are two separate processes (Duyckaerts *et al.*, 2015). Recent data indicate similar seeding activities in both Alzheimer's disease and PART beginning in the transentorhinal cortex (Kaufman *et al.*, 2018; but also see Heinsen and Grinberg, 2018). An anterior-temporal-predominant pattern of tau pathology in amyloid-β− cognitively normal older adults that is exaggerated in amyloid-β+ older adults and dementia patients is in accordance with the view that PART and Alzheimer's disease are extremes on a continuum. PET measures of amyloid-β burden revealed the opposite pattern, consistent with previous PET studies reporting predominant amyloid-β accumulation in precuneus and retrosplenial cortex/posterior cingulate cortex (Palmqvist *et al.*, 2017). Although we cannot explain the preferential accumulation of amyloid-β in posterior-medial regions of interest in the young adult/middle-aged subjects, these regions are undoubtedly the primary target of amyloid-β deposition in the progression towards Alzheimer's disease.

A behavioural shift from discrimination towards generalization in ageing has been linked to a computational bias from pattern separation towards pattern completion in the hippocampus (Wilson *et al.*, 2005). This shift has been

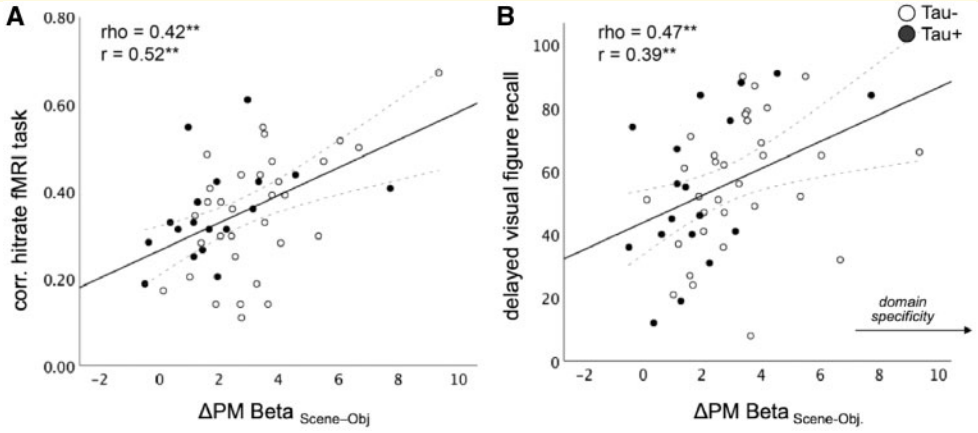

Figure 6 Lower domain-specific activation in posterior-medial regions of interest relates to worse memory in cognitively normal older adults. (**A**) Partial correlations controlling for age and gender were run within older adults ($n = 49$). Higher domain-specific activation (ΔScene – Object) in posterior-medial regions of interest was related to better functional MRI task performance (corrected hit rates) for scenes and objects. For simplicity average performance across domains is plotted here. (**B**) Higher domain-specific activation was also positively related to an independent measure of visual memory (Wechsler Memory Scale) assessed during the neuropsychological testing session. Both Spearman rank coefficient (rho) and Pearson coefficient (r) are reported. Raw data are plotted (not residuals). Mean betas were derived from FreeSurfer regions of interest in subject space. $^{*}P < 0.05$, $^{**}P < 0.01$ (uncorrected, 2-tailed).

related to loss of entorhinal input via the perforant path, as well as decreases in neurogenesis, modulatory input and inhibition (Leal and Yassa, 2018). In this sample of cognitively normal older adults, deficits in mnemonic discrimination affected—at group level—objects and scenes similarly, which replicates previous findings with our task (Berron *et al.*, 2018). However, those older individuals with more tau pathology—dominant in anterior-temporal regions—made more false alarms on object relative to scene lures, with no behavioural differences for the repeated stimuli. This suggests that effects of anterior-temporal tau pathology on behaviour in unimpaired elderly are subtle and only seen in tasks that require high precision in memory and/or perception (Barense *et al.*, 2012). Amyloid-β plaques in posterior-medial regions, which usually occur when anterior-temporal tau is already present, and which are associated with co-occurrence of tau tangles in posterior-medial regions, were related to worse scene lure discrimination. Since amyloid-β and tau pathologies are correlated but affect different memory systems, it is reasonable that relative differences in object versus scene memory are best explained when we account for both pathologies. Anterior-temporal and posterior-medial streams converge in the hippocampus where information is integrated to form episodic memories. The disturbance of both systems with the progression of Alzheimer's disease pathology might finally lead to hippocampal dysfunction that results in cognitive symptoms.

Higher activation for objects was present in anterior-temporal regions including ventral visual stream (Kravitz *et al.*, 2011) and limbic areas. In contrast, higher activity for scenes was prominent in posterior-medial regions including areas of the dorsal visual stream and default mode network (DMN; Buckner *et al.*, 2008). The posterior DMN including retrosplenial cortex/posterior cingulate cortex and precuneus constitutes a major cortical hub that is densely connected with the temporal lobe and engages in mental scene construction (Hassabis and Maguire, 2007; Andrews-Hanna *et al.*, 2010). Aberrant activity in these posterior midline regions has been reported in young adults at risk for developing Alzheimer's disease (Shine *et al.*, 2015; Hodgetts *et al.*, 2018) and in cognitively normal older adults with increased amyloid-β deposition (Sperling *et al.*, 2009). However, tau-specific PET tracers were not available in these studies. While we found only a marginal increase in posterior-medial-regional activation related to amyloid-β, high tau burden was significantly associated with elevated task activation even when accounting for amyloid-β. Since amyloid-β and tau are correlated, previous findings of amyloid-β-related hyperactivation in cognitively normal older adults might have been partially explained by tau. This is consistent with recent PET data by Huijbers *et al.* (2019) showing that increased neocortical tau burden in cognitively normal older adults relates to increased hippocampal activation during memory encoding, with no clear association seen with amyloid-β. This is also supported by data on fluid biomarkers, showing that task-related over-activation in attentional control areas (Gordon *et al.*, 2015) or diminished repetition suppression in hippocampus/amygdala (Düzel *et al.*, 2018) relates to increased CSF-tau levels but not to amyloid-β measures.

While there is clear evidence that tau and amyloid-β pathologies are related, the pathological sequence and

underlying mechanisms are unclear. In the process of protein aggregation aberrant activation might play a key role. Elevated neuronal activity stimulates the release of tau and enhances tau propagation (Yamada *et al.*, 2014; Wu *et al.*, 2016). On the other hand, tau reduction can prevent spontaneous epileptiform activity via increased inhibition in amyloid-β-overexpressing mice (Roberson *et al.*, 2007, 2011) suggesting bidirectional associations between increased activity and tau. Similarly, pathologically elevated amyloid-β destabilizes neuronal activity at the circuit and network level (Busche *et al.*, 2008; Palop and Mucke, 2010), but synaptic activity can also induce amyloid-β release (Cirrito *et al.*, 2005; Bero *et al.*, 2011). Recent data from mice expressing human amyloid-β and tau indicate complex interactions between both proteins in impairment of neural circuits integrity (Busche *et al.*, 2019) and propose that soluble tau silences neuronal activity. In our data, posterior-medial tau deposition was explained by both increased activation and amyloid-β. This is consistent with a scenario where amyloid-β accumulation initiates the spread of tau from the temporal lobe to connected posterior-medial regions via the cingulum bundle (Jacobs *et al.*, 2018), inducing aberrant activation and network disruption, further promoting tau and amyloid-β accumulation in a vicious cycle. In an alternative scenario, local tau-associated disruptions in the temporal lobe might lead to a compensatory shift of processing load to the posterior-medial system/posterior DMN, which manifests as hyperconnectivity and aberrant activation (Jones *et al.*, 2016, 2017). This could also lead to a similar vicious cycle of protein aggregation followed by cortical network failure. We do not know if amyloid-β or age-related tau deposition initiates this process. Longitudinal assessment of activation and pathology is necessary to ultimately test these hypotheses and to determine the directionality of tau-activity associations.

Our finding of reduced domain-specific activation in posterior-medial regions is also consistent with dedifferentiation theories of ageing, defined as the reduced selectivity of cortical regions sensitive to a specific class of stimuli (Park *et al.*, 2004). Age-related dedifferentiation in parahippocampal cortex in an object-scene task has been reported recently (Koen *et al.*, 2018). Our findings suggest that dedifferentiation in scene processing regions is also linked to tau deposition. Tau-associated anterior-temporal failure in old age could lead to recruitment of the posterior-medial system during object processing or tau–related disruption of the cingulum bundle might cause a failure of posterior-medial suppression. Dedifferentiation would reflect both tau-related network failure and a process that drives further protein aggregation through aberrant excitation. Functional measures of dedifferentiation have been reported to correlate negatively with cognitive performance in cognitively normal older adults (Park *et al.*, 2010; Koen *et al.*, 2018) in accordance with our results. While increased activation seems to reflect a pathological state, its functional significance varies by situation and depends on the specific brain region, the pathological stage of an individual (Celone *et al.*, 2006; Foster *et al.*, 2018) and whether the relationship is examined within or across subjects (Yassa *et al.*, 2010). While in some cases it can reflect compensation (Elman *et al.*, 2014), in our data increased task activation was detrimental. Evidence that hippocampal hyperactivation during object discrimination is not compensatory also comes from work by (Bakker *et al.*, 2012, 2015). They showed that an anti-epileptic drug reduced hippocampal hyperactivity and ameliorated behavioural deficits.

A major limitation of our study is its cross-sectional design. The acquisition of longitudinal cognitive and PET data will be necessary to ultimately determine how the progression of pathology relates to domain-specific memory deficits. We hypothesize that with ageing and accumulation of anterior-temporal tau, object discrimination declines first (Didic *et al.*, 2011; Reagh *et al.*, 2016), while with the emergence of amyloid-β and additional posterior-medial tau, scene discrimination performance decreases later, leading to more severe memory deficits. This suggests that within-subject changes in object and scene discrimination may be most sensitive to predict disease progression. We note that our sample is a selective group of highly educated cognitively normal older adults that included an increased proportion of amyloid-β+ individuals with 50% (expected probability 20–35%; Ossenkoppele *et al.*, 2015). However, this feature of the study enhanced our ability to differentiate associations with tau from the influence of amyloid-β. Furthermore, we only included late-onset patients with amnestic manifestations and the majority of our patients were mildly impaired. Thus our findings cannot be generalized and it is possible that patients who are younger or further progressed on the Alzheimer's disease trajectory show a shift towards higher posterior-medial than anterior-temporal tau accumulation. Our analyses on a combined anterior-temporal region of interest did also not provide evidence for reduced object activation (Berron *et al.*, 2017; Reagh *et al.*, 2018) but we have not yet considered all medial temporal lobe subdivisions that are discernible with MRI (e.g. anterior lateral entorhinal cortex, area 35 or 36). It is also likely that anterior-temporal and posterior-medial regions that were not covered by our *a priori* regions of interest due to methodological reasons contribute to our findings, and moreover it is possible that pathology in other brain networks affects domain-specific discrimination. Finally, we want to point out that although anterior-temporal or posterior-medial regions show preferential engagement for one domain over the other, these cortical streams are interconnected and not exclusively involved in processing of one domain (Connor and Knierim, 2017; Burke *et al.*, 2018). However, with this complexity in mind, it is even more striking that a dissociation of behavioural deficits in relationship to tau and amyloid-β pathologies was evident.

These findings demonstrate continuity between ageing and Alzheimer's disease, and implicate hyperactivation in

the pathway from protein aggregation to cognitive decline. They further suggest that anatomically targeted memory tests can detect the earliest and subtle cognitive signs of Alzheimer's disease and improve assessment for pathology-specific therapeutic approaches including those targeting hyperexcitability. Longitudinal studies will help define the clinical utility and predictive value of these observations.

Acknowledgements

Avid Radiopharmaceuticals enabled use of the ^{18}F-FTP tracer, but did not provide direct funding and were not involved in data analysis or interpretation.

Funding

This research was funded by the Helmholtz Postdoc Program [PD-306] (to A.M.), Tau Consortium (to W.J.J. and G.D.R.), National Institute on Aging grants [R01-AG034570] (to W.J.J.), [P50-AG023501] (G.D.R.), F32-AG05710 (to T.M.H.), AARF-16–443577 (to R.L.J.), SFB 776/TP A07 und Human Brain Project SP3/WP3.3.1 (to E.D.).

Competing interests

W.J.J. has served as a consultant to Genentech, Novartis, and Bioclinica. Dr Düzel has served as a consultant to Heptares. E.D. and D.B. are scientific co-founders of neotiv GmbH. All other authors report no disclosures.

Supplementary material

Supplementary material is available at *Brain* online.

References

Albert MS, DeKosky ST, Dickson D, Dubois B, Feldman HH, Fox NC, et al. The diagnosis of mild cognitive impairment due to Alzheimer's disease: recommendations from the National Institute on Aging-Alzheimer's Association workgroups on diagnostic guidelines for Alzheimer's disease. Alzheimers Dement 2011; 7: 270–9.

Andrews-Hanna JR, Reidler JS, Sepulcre J, Poulin R, Buckner RL. Functional-anatomic fractionation of the brain's default network. Neuron 2010; 65: 550–62.

Baker SL, Maass A, Jagust WJ. Considerations and code for partial volume correcting [18F]-AV-1451 tau PET data. Data Brief 2017; 15: 648–57.

Bakker A, Albert MS, Krauss G, Speck CL, Gallagher M. Response of the medial temporal lobe network in amnestic mild cognitive impairment to therapeutic intervention assessed by fMRI and memory task performance. NeuroImage Clin 2015; 7: 688–98.

Bakker A, Krauss GL, Albert MS, Speck CL, Jones LR, Stark CE, et al. Reduction of hippocampal hyperactivity improves cognition in amnestic mild cognitive impairment. Neuron 2012; 74: 467–74.

Barense MD, Groen IIA, Lee ACH, Yeung L-K, Brady SM, Gregori M, et al. Intact memory for irrelevant information impairs perception in amnesia. Neuron 2012; 75: 157–67.

Bero AW, Yan P, Roh JH, Cirrito JR, Stewart FR, Raichle ME, et al. Neuronal activity regulates the regional vulnerability to amyloid-β deposition. Nat Neurosci 2011; 14: 750–76.

Berron D, Neumann K, Maass A, Schütze H, Fliessbach K, Kiven V, et al. Age-related functional changes in domain-specific medial temporal lobe pathways. Neurobiol Aging 2018; 65: 86–97.

Berron D, Vieweg P, Hochkeppler A, Pluta JB, Ding S-L, Maass A, et al. A protocol for manual segmentation of medial temporal lobe subregions in 7 Tesla MRI. NeuroImage Clin 2017; 15: 466–42.

Braak H, Braak E. Frequency of stages of Alzheimer-related lesions in different age categories. Neurobiol Aging 1997; 18: 351–7.

Buckner RL, Andrews-Hanna JR, Schacter DL. The brain's default network: anatomy, function, and relevance to disease. Ann N Y Acad Sci 2008; 1124: 1–38.

Burke SN, Gaynor LS, Barnes CA, Bauer RM, Bizon JL, Roberson ED, et al. Shared functions of perirhinal and parahippocampal cortices: implications for cognitive aging. Trends Neurosci 2018. Available from: http://www.cell.com/trends/neurosciences/abstract/S0166–2236 (19 March 2018, date last accessed).

Burke SN, Ryan L, Barnes CA. Characterizing cognitive aging of recognition memory and related processes in animal models and in humans. Front Aging Neurosci 2012; 4: 15.

Busche MA, Eichhoff G, Adelsberger H, Abramowski D, Wiederhold K-H, Haass C, et al. Clusters of hyperactive neurons near amyloid plaques in a mouse model of Alzheimer's disease. Science 2008; 321: 1686–9.

Busche MA, Wegmann S, Dujardin S, Commins C, Schiantarelli J, Klickstein N, et al. Tau impairs neural circuits, dominating amyloid-β effects, in Alzheimer models in vivo. Nat Neurosci 2019; 22: 57.

Celone KA, Calhoun VD, Dickerson BC, Atri A, Chua EF, Miller SL, et al. Alterations in memory networks in mild cognitive impairment and Alzheimer's disease: an independent component analysis. J Neurosci 2006; 26: 10222–31.

Cirrito JR, Yamada KA, Finn MB, Sloviter RS, Bales KR, May PC, et al. Synaptic activity regulates interstitial fluid amyloid-beta levels in vivo. Neuron 2005; 48: 913–22.

Connor CE, Knierim JJ. Integration of objects and space in perception and memory. Nat Neurosci 2017; 20: 1493–503.

Cope TE, Rittman T, Borchert RJ, Jones PS, Vatansever D, Allinson K, et al. Tau burden and the functional connectome in Alzheimer's disease and progressive supranuclear palsy. Brain J Neurol 2018; 141: 550–67.

Crary JF, Trojanowski JQ, Schneider JA, Abisambra JF, Abner EL, Alafuzoff I, et al. Primary age-related tauopathy (PART): a common pathology associated with human aging. Acta Neuropathol 2014; 128: 755–66.

Didic M, Barbeau EJ, Felician O, Tramoni E, Guedj E, Poncet M, et al. Which memory system is impaired first in Alzheimer's disease? J Alzheimers Dis 2011; 27: 11–22.

Duyckaerts C, Braak H, Brion J-P, Buée L, Del Tredici K, Goedert M, et al. PART is part of Alzheimer disease. Acta Neuropathol 2015; 129: 749–56.

Düzel E, Berron D, Schütze H, Cardenas-Blanco A, Metzger C, Betts M, et al. CSF total tau levels are associated with hippocampal novelty irrespective of hippocampal volume. Alzheimers Dement 2018. Available from: http://www.sciencedirect.com/science/article/pii/S235287291830071X (17 November 2018, date last accessed).

Elman JA, Oh H, Madison CM, Baker SL, Vogel JW, Marks SM, et al. Neural compensation in older people with brain β-amyloid deposition. Nat Neurosci 2014; 17: 1316–8.

Foster CM, Kennedy KM, Horn MM, Hoagey DA, Rodrigue KM. Both hyper- and hypo-activation to cognitive challenge are associated with increased beta-amyloid deposition in healthy aging: a nonlinear effect. NeuroImage 2018; 166: 285–92.

Franzmeier N, Rubinski A, Neitzel J, Kim Y, Damm A, Na DL, et al. Functional connectivity associated with tau levels in ageing, Alzheimer's, and small vessel disease. Brain 2019; 142: 1093–107.

Giannakopoulos P, Herrmann FR, Bussière T, Bouras C, Kövari E, Perl DP, et al. Tangle and neuron numbers, but not amyloid load, predict cognitive status in Alzheimer's disease. Neurology 2003; 60: 1495–500.

Gordon BA, Zacks JM, Blazey T, Benzinger TL, Morris JC, Fagan AM, et al. Task-evoked fMRI changes in attention networks are associated with preclinical Alzheimer Disease biomarkers. Neurobiol Aging 2015; 36: 1771–9.

Hassabis D, Maguire EA. Deconstructing episodic memory with construction. Trends Cogn Sci 2007; 11: 299–306.

Heinsen H, Grinberg LT. On the origin of tau seeding activity in Alzheimer's disease. Acta Neuropathol 2018. Advance Access published on September 6, 2018, doi:10.1007/s00401–018–1890–3.

Hodgetts CJ, Shine JP, Williams H, Postans M, Sims R, Williams J, et al. Increased posterior default mode network activity and structural connectivity in young adult APOE-ε4 carriers: a multi-modal imaging investigation. Neurobiol Aging 2018. Available from: http://www.sciencedirect.com/science/article/pii/S0197458018303348 (11 October 2008, date last accessed).

Huijbers W, Mormino EC, Wigman SE, Ward AM, Vannini P, McLaren DG, et al. Amyloid deposition is linked to aberrant entorhinal activity among cognitively normal older adults. J Neurosci 2014; 34: 5200–10.

Huijbers W, Schultz AP, Papp KV, LaPoint MR, Hanseeuw B, Chhatwal JP, et al. Tau accumulation in clinically normal older adults is associated with hippocampal hyperactivity. J Neurosci 2019; 39: 548–56.

Inhoff MC, Ranganath C. Dynamic cortico-hippocampal networks underlying memory and cognition: The PMAT framework. In: Hannula DE, Duff MC, editors. The hippocampus from cells to systems: Structure, connectivity, and functional contributions to memory and flexible cognition. Cham, Switzerland: Springer International Publishing; 2017. p. 559–89.

Jack CR, Bennett DA, Blennow K, Carrillo MC, Dunn B, Haeberlein SB, et al. NIA-AA research framework: toward a biological definition of Alzheimer's disease. Alzheimers Dement 2018; 14: 535–62.

Jacobs HIL, Hedden T, Schultz AP, Sepulcre J, Perea RD, Amariglio RE, et al. Structural tract alterations predict downstream tau accumulation in amyloid-positive older individuals. Nat Neurosci 2018; 21: 424–31.

Jones DT, Graff-Radford J, Lowe VJ, Wiste HJ, Gunter JL, Senjem ML, et al. Tau, amyloid, and cascading network failure across the Alzheimer's disease spectrum. Cortex 2017; 97: 143–59.

Jones DT, Knopman DS, Gunter JL, Graff-Radford J, Vemuri P, Boeve BF, et al. Cascading network failure across the Alzheimer's disease spectrum. Brain J Neurol 2016; 139: 547–62.

Kaufman SK, Del Tredici K, Thomas TL, Braak H, Diamond MI. Tau seeding activity begins in the transentorhinal/entorhinal regions and anticipates phospho-tau pathology in Alzheimer's disease and PART. Acta Neuropathol 2018; 136: 57–67.

Kfoury N, Holmes BB, Jiang H, Holtzman DM, Diamond MI. Trans-cellular propagation of Tau aggregation by fibrillar species. J Biol Chem 2012; 287: 19440–51.

Kim S, Nilakantan AS, Hermiller MS, Palumbo RT, VanHaerents S, Voss JL. Selective and coherent activity increases due to stimulation indicate functional distinctions between episodic memory networks. Sci Adv 2018; 4: eaar2768.

Koen JD, Hauck N, Rugg MD. The relationship between age, neural differentiation, and memory performance. J Neurosci 2018; 39: 149–62.

Kravitz DJ, Saleem KS, Baker CI, Mishkin M. A new neural framework for visuospatial processing. Nat Rev Neurosci 2011; 12: 217–30.

Leal SL, Landau SM, Bell RK, Jagust WJ. Hippocampal activation is associated with longitudinal amyloid accumulation and cognitive decline. eLife 2017; 6 doi: 10.7554/eLife.22978.

Leal SL, Lockhart SN, Maass A, Bell RK, Jagust WJ. Subthreshold amyloid predicts tau deposition in aging. J Neurosci 2018; 38: 4482–89.

Leal SL, Yassa MA. Integrating new findings and examining clinical applications of pattern separation. Nat Neurosci 2018; 21: 163–73.

Lockhart SN, Schöll M, Baker SL, Ayakta N, Swinnerton KN, Bell RK, et al. Amyloid and tau PET demonstrate region-specific associations in normal older people. NeuroImage 2017; 150: 191–9.

Logan J, Fowler JS, Volkow ND, Wang GJ, Ding YS, Alexoff DL. Distribution volume ratios without blood sampling from graphical analysis of PET data. J Cereb Blood Flow Metab 1996; 16: 834–40.

Maass A, Berron D, Libby L, Ranganath C, Düzel E. Functional subregions of the human entorhinal cortex. eLife 2015; 4. doi: 10.7554/eLife.06426.

Maass A, Landau S, Baker SL, Horng A, Lockhart SN, La Joie R, et al. Comparison of multiple tau-PET measures as biomarkers in aging and Alzheimer's Disease. NeuroImage 2017; 157: 448–63.

Maass A, Lockhart SN, Harrison TM, Bell RK, Mellinger T, Swinnerton K, et al. Entorhinal tau pathology, episodic memory decline and neurodegeneration in aging. J Neurosci 2018; 38: 530–43.

Marks SM, Lockhart SN, Baker SL, Jagust WJ. Tau and β-amyloid are associated with medial temporal lobe structure, function, and memory encoding in normal aging. J Neurosci 2017; 37: 3192–201.

McKhann GM, Knopman DS, Chertkow H, Hyman BT, Jack CR, Kawas CH, et al. The diagnosis of dementia due to Alzheimer's disease: recommendations from the National Institute on Aging-Alzheimer's Association workgroups on diagnostic guidelines for Alzheimer's disease. Alzheimers Dement 2011; 7: 263–9.

Mormino EC, Brandel MG, Madison CM, Marks S, Baker SL, Jagust WJ. Aβ deposition in aging is associated with increases in brain activation during successful memory encoding. Cereb Cortex 2011. Available from: http://www.ncbi.nlm.nih.gov/pubmed/21945849 (20 April 2012, date last accessed).

Mormino EC, Brandel MG, Madison CM, Rabinovici GD, Marks S, Baker SL, et al. Not quite PIB-positive, not quite PIB-negative: slight PIB elevations in elderly normal control subjects are biologically relevant. NeuroImage 2012; 59: 1152–60.

Oh H, Madison C, Baker S, Rabinovici G, Jagust W. Dynamic relationships between age, amyloid-β deposition, and glucose metabolism link to the regional vulnerability to Alzheimer's disease. Brain J Neurol 2016; 139: 2275–89.

Oh H, Steffener J, Razlighi QR, Habeck C, Liu D, Gazes Y, et al. Aβ-related hyperactivation in frontoparietal control regions in cognitively normal elderly. Neurobiol Aging 2015; 36: 3247–54.

Olsen RK, Yeung L-K, Noly-Gandon A, D'Angelo MC, Kacollja A, Smith VM, et al. Human anterolateral entorhinal cortex volumes are associated with cognitive decline in aging prior to clinical diagnosis. Neurobiol Aging 2017; 57: 195–205.

Ossenkoppele R, Jansen WJ, Rabinovici GD, Knol DL, van der Flier WM, van Berckel BNM, et al. Prevalence of amyloid PET positivity in dementia syndromes: a meta-analysis. JAMA 2015; 313: 1939–49.

Ossenkoppele R, Schonhaut DR, Schöll M, Lockhart SN, Ayakta N, Baker SL, et al. Tau PET patterns mirror clinical and neuroanatomical variability in Alzheimer's disease. Brain 2016; 139: 1551–67.

Palmqvist S, Schöll M, Strandberg O, Mattsson N, Stomrud E, Zetterberg H, et al. Earliest accumulation of β-amyloid occurs within the default-mode network and concurrently affects brain connectivity. Nat Commun 2017; 8: 1214.

Palop JJ, Mucke L. Amyloid-β-induced neuronal dysfunction in Alzheimer's disease: from synapses toward neural networks. Nat Neurosci 2010; 13: 812–8.

Park DC, Polk TA, Park R, Minear M, Savage A, Smith MR. Aging reduces neural specialization in ventral visual cortex. Proc Natl Acad Sci USA 2004; 101: 13091–5.

Park J, Carp J, Hebrank A, Park DC, Polk TA. Neural specificity predicts fluid processing ability in older adults. J Neurosci 2010; 30: 9253–9.

Price JC, Klunk WE, Lopresti BJ, Lu X, Hoge JA, Ziolko SK, et al. Kinetic modeling of amyloid binding in humans using PET imaging and Pittsburgh compound-B. J Cereb Blood Flow Metab 2005; 25: 1528–47.

Ranganath C, Ritchey M. Two cortical systems for memory-guided behaviour. Nat Rev Neurosci 2012; 13: 713–26.

Reagh ZM, Ho HD, Leal SL, Noche JA, Chun A, Murray EA, et al. Greater loss of object than spatial mnemonic discrimination in aged adults. Hippocampus 2016; 26: 417–22.

Reagh ZM, Noche JA, Tustison NJ, Delisle D, Murray EA, Yassa MA. Functional imbalance of anterolateral entorhinal cortex and hippocampal dentate/CA3 underlies age-related object pattern separation deficits. Neuron 2018; 97: 1187–98.e4.

Roberson ED, Halabisky B, Yoo JW, Yao J, Chin J, Yan F, et al. Amyloid-β/Fyn-induced synaptic, network, and cognitive impairments depend on tau levels in multiple mouse models of Alzheimer's disease. J Neurosci 2011; 31: 700–11.

Roberson ED, Scearce-Levie K, Palop JJ, Yan F, Cheng IH, Wu T, et al. Reducing endogenous tau ameliorates amyloid beta-induced deficits in an Alzheimer's disease mouse model. Science 2007; 316: 750–4.

Rousset OG, Ma Y, Evans AC. Correction for partial volume effects in PET: principle and validation. J Nucl Med 1998; 39: 904–11.

Schöll M, Lockhart SN, Schonhaut DR, O'Neil JP, Janabi M, Ossenkoppele R, et al. PET Imaging of tau deposition in the aging human brain. Neuron 2016; 89: 971–82.

Schröder TN, Haak KV, Jimenez NIZ, Beckmann CF, Doeller CF. Functional topography of the human entorhinal cortex. eLife 2015; 4: e06738.

Shine JP, Hodgetts CJ, Postans M, Lawrence AD, Graham KS. APOE-ε4 selectively modulates posteromedial cortex activity during scene perception and short-term memory in young healthy adults. Sci Rep 2015; 5: 16322.

Sperling RA, LaViolette PS, O'Keefe K, O'Brien J, Rentz DM, Pihlajamaki M, et al. Amyloid deposition is associated with impaired default network function in older persons without dementia. Neuron 2009; 63: 178–88.

Todd N, Moeller S, Auerbach EJ, Yacoub E, Flandin G, Weiskopf N. Evaluation of 2D multiband EPI imaging for high-resolution, whole-brain, task-based fMRI studies at 3T: sensitivity and slice leakage artifacts. NeuroImage 2015; 124: 32–42.

Vannini P, Hedden T, Becker JA, Sullivan C, Putcha D, Rentz D, et al. Age and amyloid-related alterations in default network habituation to stimulus repetition. Neurobiol Aging 2012; 33: 1237–52.

Vemuri P, Lowe VJ, Knopman DS, Senjem ML, Kemp BJ, Schwarz CG, et al. Tau-PET uptake: Regional variation in average SUVR and impact of amyloid deposition. Alzheimers Dement 2017; 6: 21–30.

Villeneuve S, Rabinovici GD, Cohn-Sheehy BI, Madison C, Ayakta N, Ghosh PM, et al. Existing Pittsburgh compound-B positron emission tomography thresholds are too high: statistical and pathological evaluation. Brain J Neurol 2015; 138: 2020–33.

Wilson IA, Gallagher M, Eichenbaum H, Tanila H. Neurocognitive aging: prior memories hinder new hippocampal encoding. Trends Neurosci 2006; 29: 662–70.

Wilson IA, Ikonen S, Gallagher M, Eichenbaum H, Tanila H. Age-associated alterations of hippocampal place cells are subregion specific. J Neurosci 2005; 25: 6877–86.

Wu JW, Hussaini SA, Bastille IM, Rodriguez GA, Mrejeru A, Rilett K, et al. Neuronal activity enhances tau propagation and tau pathology in vivo. Nat Neurosci 2016; 19: 1085–92.

Xie L, Das SR, Wisse LEM, Ittyerah R, Yushkevich PA, Wolk DA. Early tau burden correlates with higher rate of atrophy in transentorhinal cortex. J Alzheimers Dis 2018; 62: 85–92.

Yamada K, Holth JK, Liao F, Stewart FR, Mahan TE, Jiang H, et al. Neuronal activity regulates extracellular tau in vivo. J Exp Med 2014; 211: 387–93.

Yassa MA, Stark SM, Bakker A, Albert MS, Gallagher M, Stark CEL. High-resolution structural and functional MRI of hippocampal CA3 and dentate gyrus in patients with amnestic mild cognitive impairment. NeuroImage 2010; 51: 1242–52.

Yeung L-K, Olsen RK, Bild-Enkin HEP, D'Angelo MC, Kacollja A, McQuiggan DA, et al. Anterolateral entorhinal cortex volume predicted by altered intra-item configural processing. J Neurosci 2017; 37: 5527–38.